

# Realization of Regular-Mixed Quasi-1D Borophene Chains with Long-Range Order

Yu Wang, Longjuan Kong, Caiyun Chen, Peng Cheng, Baojie Feng, Kehui Wu,\*  
and Lan Chen\*

The polymorphism of borophene makes it a promising system to realize tunable physical or chemical properties. Various pure borophene phases consisting of quasi-1D boron chains with different widths have been commonly obtained in experimental studies. Here, it is shown that, due to a substrate mediation effect, artificial long-range ordered phases of borophene consisting of different combinations of boron chains seamlessly joined together can be achieved on Ag(100). Scanning tunneling microscopy measurements and theoretical calculations reveal that mixed-chain phases are more stable than the pure phase, and interact only weakly with the substrate. The mixed-chain phases with various proportions of different chains can be well separated based on the crystal direction of the substrate. The successful growth of mixed-chain phases is expected to deepen the impact of substrate tailored synthesis of borophene.

Recently, monoelemental 2D materials beyond graphene<sup>[1–9]</sup> have been widely investigated experimentally and theoretically due to their non-trivial physical properties and fascinating potential for future application in nanoscale devices. In particular, the 2D sheet of boron atoms arranged in a triangular lattice with hexagonal holes named borophene has sparked an enormous research effort<sup>[10,11]</sup> including theoretical predictions of its properties<sup>[12–20]</sup> and its experimental preparation on metal surfaces.<sup>[21–28]</sup> Extraordinary properties of borophene have been reported, such as 1D nearly free electron states,<sup>[29]</sup> presence of

metallic Dirac fermions,<sup>[30–32]</sup> predicted superconductivity,<sup>[33]</sup> high mechanical flexibility,<sup>[34]</sup> and high thermal conductivity.<sup>[35]</sup>

The complexity of chemical bonds due to the electronic deficiency in boron atoms can induce polymorphism in borophene,<sup>[13,36,37]</sup> so that the different arrangements of hexagonal holes in the borophene triangular lattice result in the various atomic borophene structures.<sup>[12,15,16]</sup> The pure phases of borophene on Ag(111) consist of quasi-1D boron chains with different widths with the (2,3) chains in the  $\beta_{12}$  or  $\nu_{1/6}$  sheets and the (2,2) chains in the  $\chi_3$  or  $\nu_{1/5}$  sheets.<sup>[20,22,23]</sup> Here, in  $(n, m)$ ,  $n$  and  $m$  denote the number of atoms in the widest and narrowest regions of a single boron chain.<sup>[24]</sup> More importantly, it

has been observed that different types of quasi-1D boron chains can intermix with each other at the domain boundaries of different borophene phases.<sup>[38,39]</sup> Inspired by this phenomenon, we hypothesize that quasi-1D boron chains may act as building blocks that can be mixed together to form novel artificial borophene phases, enriching the diversity of borophene phases and giving rise to novel physical properties. For example, a honeycomb borophene lattice may enable the simultaneous presence of Dirac fermions and superconductivity.<sup>[40]</sup> Therefore, it is highly important to experimentally realize mixed-chain phases with long-range order.


Previous studies of borophene fabrication on metal surfaces have suggested that the structures and morphologies of borophene can be modified by borophene-metal interface interactions such as lattice matching<sup>[22,41]</sup> and charge transfer.<sup>[25,42]</sup> Here, we report the successful growth of borophene on the Ag(100) surface carried out using the molecular beam epitaxy (MBE) method. Combining scanning tunneling microscopy (STM) and first-principles calculations, we have obtained three phases of borophene and identified two long-range ordered phases of them with different proportions of (2,3) and (2,2) boron chains. Detailed analysis revealed that modulation of the interface interactions between borophene and the Ag(100) surface due to lattice matching and the orientation of the boron chains relative to the substrate play important roles in the formation of these two mixed-chain phases. As a result, the two mixed-chain phases can be well separated based on the crystal orientation of the substrate. Our results are consistent with the polymorphism in borophene, and provide a promising approach for the fabricating novel borophene phases through substrate modulation.

Y. Wang, Dr. L. Kong, C. Chen, Prof. P. Cheng, Prof. B. Feng, Prof. K. Wu,  
Prof. L. Chen  
Institute of Physics  
Chinese Academy of Sciences  
Beijing 100190, China  
E-mail: khwu@iphy.ac.cn; lchen@iphy.ac.cn

Y. Wang, Dr. L. Kong, C. Chen, Prof. P. Cheng, Prof. B. Feng, Prof. K. Wu,  
Prof. L. Chen  
School of Physical Sciences  
University of Chinese Academy of Sciences  
Beijing 100190, China

Dr. L. Kong  
School of Physics  
Nankai University  
Tianjin 300071, China

Prof. K. Wu, Prof. L. Chen  
Songsan Lake Materials Laboratory  
Dongguan 523808, China

 The ORCID identification number(s) for the author(s) of this article can be found under <https://doi.org/10.1002/adma.202005128>.

DOI: 10.1002/adma.202005128

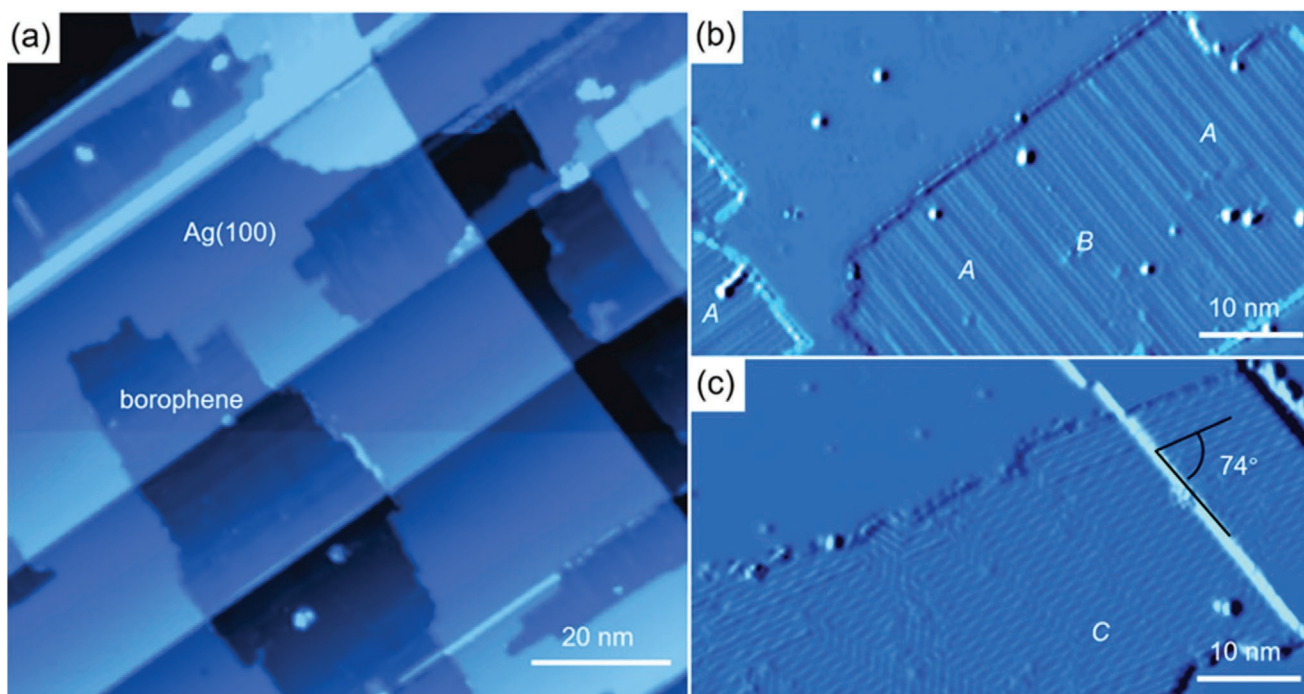


**Figure 1.** Monolayer borophene on Ag(100). a) STM image of borophene grown at 550 K on the Ag(100) surface (100 nm  $\times$  100 nm;  $V_t = -1$  V,  $I_t = 70$  pA). The bright area is the Ag surface, while the dark areas are borophene islands. b,c) Differential STM images of types I and II borophene islands, respectively (60 nm  $\times$  30 nm;  $V_t = -1$  V,  $I_t = 200$  pA for (b);  $V_t = -0.4$  V,  $I_t = 70$  pA for (c)). Boron chains (type I) arrange along the crystal direction [110] of Ag(100), and type II islands contain parallel chains oriented at an angle of 74° with respect to the [110] direction of Ag(100). The letters A, B, and C are used to indicate the three different 2D boron phases.

**Figure 1a** shows a typical STM topographic image of an  $\approx 0.5$  monolayer (ML) of boron atoms deposited on the Ag(100) surface. We found that half of the surface is covered by dark islands that run continuously across the steps of the Ag(100) substrate, indicating the formation of borophene. A closer examination reveals that two types of islands are present on the Ag(100) surface: type I islands consist of parallel chains along the high-symmetry [110] direction of Ag(100) (Figure 1b), and type II islands contain parallel chains rotated by 74° with respect to the [110] direction of Ag(100) (Figure 1c). Furthermore, type I islands exhibit two different forms: the majority form has brighter parallel chains (named phase A), and the minority form has darker parallel chains (phase B). Overall, three different phases of borophene are formed on the Ag(100) surface, namely phases A and B in type I islands, and phase C in type II islands.

The high-resolution STM images of phases A and B are shown in **Figures 2a,b**, respectively. It is clearly observed that phase A consists of alternating bright double-chains and dark single-chains, while phase B consists of four parallel chains with different brightness levels. Based on the STM images, the lattice constants for the two phases are obtained as  $28.8 \pm 0.4$  Å  $\times$   $2.9 \pm 0.1$  Å (A) and  $20.0 \pm 0.3$  Å  $\times$   $2.9 \pm 0.1$  Å (B), respectively. In both phases, the distance between the neighboring nodes along the chains coincides with the lattice constant of Ag(100) (2.89 Å), while the average lateral distances between the neighbor chains are 4.8 and 5.0 Å for phases A and B, respectively. According to the previous works on the synthesis of borophene on Ag(111), the (2,3) chains in the  $\beta_{12}$

sheet and the (2,2) chains in the  $\chi_3$  sheet have the same period along the chains (2.9 Å), while the lateral distances between the neighbor chains are 5.0 and 4.3 Å, respectively. Therefore, it is reasonable to assume that A is the boron phase with four (2,3) and two (2,2) chains mixed in a single unit cell [(2,3):(2,2) = 2:1], and B is the pure  $\beta_{12}$  phase consisting of (2,3) chains.

To confirm these models, we performed first-principles calculations on the mixed-chain phase A and pure  $\beta_{12}$ -sheet (phase B) on the Ag(100) substrate. All of the chains are oriented along the [110] direction of the Ag(100), as shown in Figure 2e,f. After relaxation, the overall structures of the mixed-chain phase and the pure  $\beta_{12}$ -sheet remain intact and planar, suggesting that both models are stable. It is noted that due to the lattice mismatch between borophene and Ag(100), three times the average lateral distance between the neighbor chains in phase A ( $4.8$  Å  $\times$   $3 = 14.4$  Å) is quite close to five times the lattice parameter of Ag(100) ( $5 \times 2.89$  Å  $\approx 14.5$  Å), while four times the lateral distance between the neighbor chains in B ( $5.0$  Å  $\times$   $4 = 20.0$  Å) almost matches seven times the lattice parameter of Ag(100) ( $7 \times 2.89$  Å  $\approx 20.2$  Å). This means that moiré patterns with the periodicities of 14.4 and 20.0 Å will form along the lateral direction of the boron chains. The simulated STM images shown in Figure 2c,d reproduce the alternating brighter double-chains and dark single-chains in the mixed-chain phase A, as well as four kinds of parallel chains with different brightness in the pure  $\beta_{12}$ -sheet, showing full agreement with the experimental STM images.

As shown in **Figure 3a**, the high-resolution STM image of phase C exhibits alternating brighter single-chains and darker



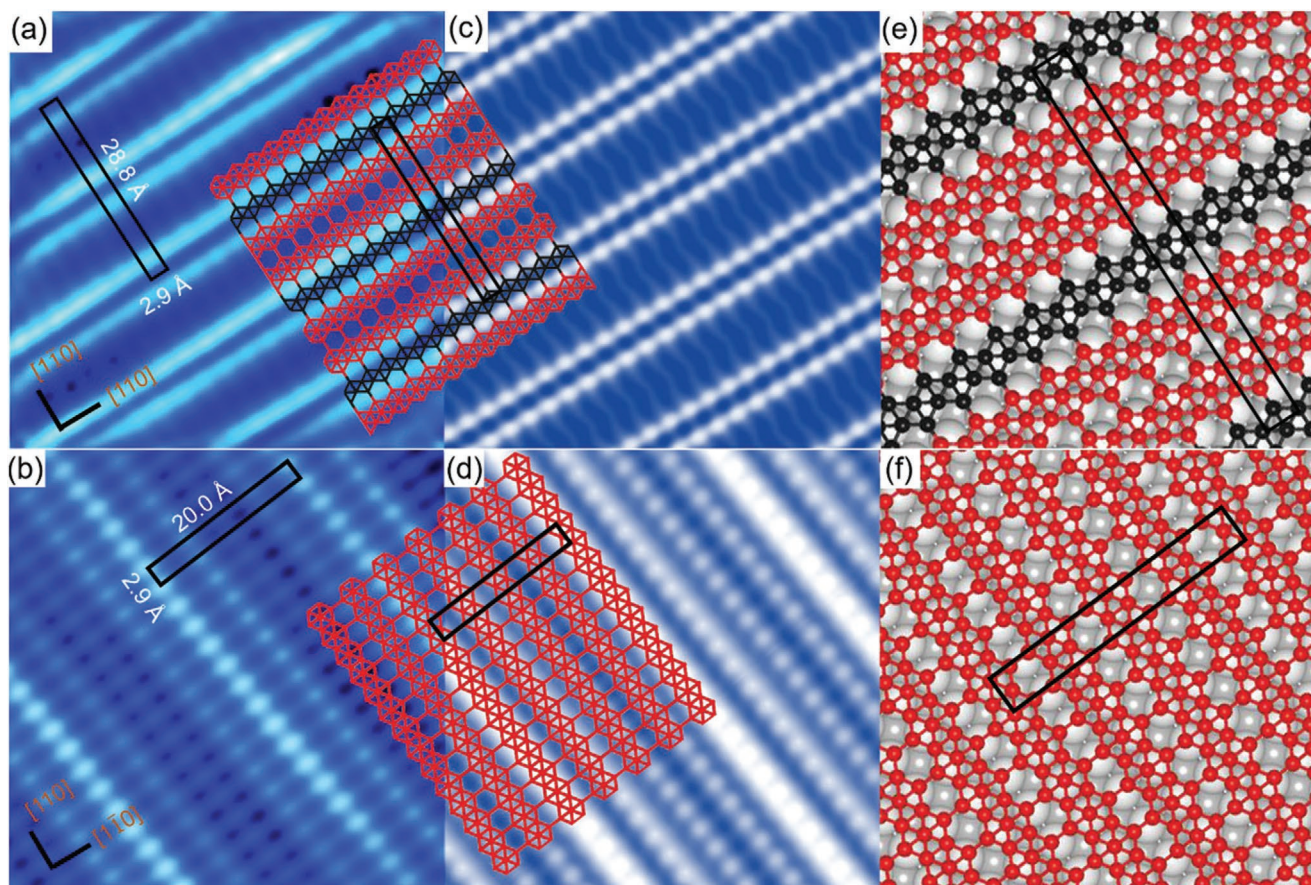


**Figure 2.** Borophene phases on type I islands. a) STM image of phase A ( $5 \text{ nm} \times 5 \text{ nm}$ ;  $V_t = -1 \text{ V}$ ,  $I_t = 70 \text{ pA}$ ). b) STM image of phase B ( $5 \text{ nm} \times 5 \text{ nm}$ ;  $V_t = -0.5 \text{ V}$ ,  $I_t = 200 \text{ pA}$ ). c,d) Simulated STM images of phases A and B with overlaid atomic model, respectively. e,f) Atomic configurations of phases A and B, respectively. The red and black spheres represent boron atoms in different kinds of chains, respectively. The white spheres represent the silver atoms in the top Ag(100) layer. For clarity, the Ag atoms of the second Ag(100) layer are shown in light gray. The unit cells are indicated by the black rectangles.

double-chains. Unlike for phases A and B, the period of the nodes along the chains in phase C is approximately  $12.0 \pm 0.2 \text{ \AA}$ , which is about four times greater than the smallest period along

the (2,3) and (2,2) chains. On the other hand, the average distance between the neighboring chains is approximately  $4.5 \text{ \AA}$ , which is smaller than that in phase A but larger than that

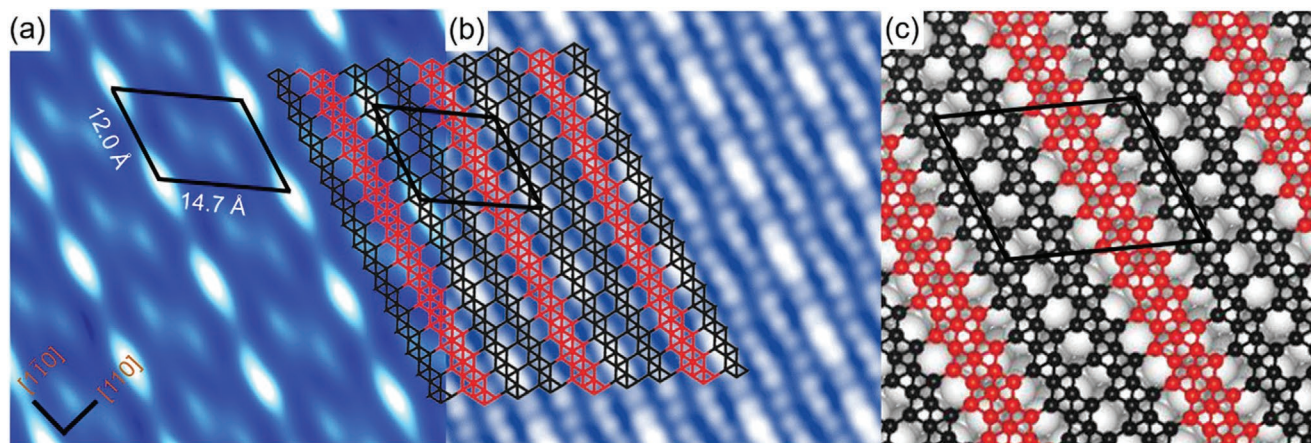


**Figure 3.** Borophene phases on type II islands. a) STM image of phase C ( $5 \text{ nm} \times 5 \text{ nm}$ ;  $V_t = -0.1 \text{ V}$ ,  $I_t = 50 \text{ pA}$ ). b) Simulated STM image of phase C. c) Atomic configuration of phase C. The simulated STM image in (b) is superimposed by atomic models. The red and black spheres represent boron atoms in different kinds of chains, respectively. The white spheres represent the silver atoms of the top Ag(100) layer. For clarity, the Ag atoms of the top Ag(100) layer are shown in light gray. The unit cells are indicated by the black parallelograms.



between the (2,2) chains in the  $\chi_3$  sheet on Ag(111). Therefore, it is likely that phase C consists of one (2,3) and two (2,2) chains in a single unit cell, and the ratio of the (2,3) and (2,2) chains is lower than that for phase A [(2,3):(2,2) = 2:1]. To confirm this model, first-principles calculations were performed for this model on the Ag(100) substrate, where all of the chains are rotated by 74° with respect to the [110] direction of Ag(100), as shown in Figure 3c. After relaxation, the global structure of the mixed chain phase remains intact and planar, suggesting the stability of our model. The simulated STM images shown in Figure 3b are in full agreement with the experimental STM image and perfectly match the features of the mixed-chain phase C.

Combining the above experimental and theoretical results, we can conclude that long-range ordered mixed-chain phases have been realized on the Ag(100) surface. More importantly, the mixed-chain phases with different proportions of different chains can be well separated based on the crystal orientations of the substrate. Next, we will discuss the mechanism for the formation of the mixed-chain phases on Ag(100).

First, DFT calculations were performed to determine the formation energies of the different borophene phases on the Ag(100) surface. The structural stability of different phases can be estimated based on their formation energy,  $E_f = (E_{\text{tot}} - E_{\text{sub}} - N \times E_B)/N$ , where  $E_{\text{tot}}$  is the total energy of the monolayer borophene on the metal substrate,  $E_{\text{sub}}$  is the total energy of the substrate,  $E_B$  is the energy per atom of the solid  $\alpha$  phase boron, and  $N$  is the number of boron atoms in each unit cell.<sup>[17]</sup> As illustrated in the Table 1, the calculated formation energy is 0.262 eV/atom for mixed-chain phase A (the hole density is 3/17), and 0.266 eV/atom for mixed-chain phase C (the hole density is 3/16), both of which are lower than that of phase B (pure  $\beta_{12}$  phase) (0.272 eV/atom), and are even lower than that of pure  $\beta_{12}$  on Ag(111). This provides a satisfactory explanation for the formation of the mixed-chain phases in large areas on Ag(100). Moreover, the hole densities of the mixed-chain phases A and C are 3/17 and 3/16, which are slightly larger than that of pure phase B (1/6).

To examine the interactions at the borophene-Ag(100) interface, we calculated the charge transfer between the borophene films and the Ag(100) surface (see Table 1). The amount of electrons transferred from the Ag(100) surface was found to be 0.019, 0.019, and 0.022 electron per boron atom for phases A, B, and C, respectively. The values of the charge transfer from Ag(100) to the boron sheets is even smaller than that of the pure phases on Ag(111) (0.03 and 0.022 electron per boron

atom for phases  $\beta_{12}$  and  $\chi_3$ , respectively), reflecting the weaker boron–metal interactions in the B/Ag(100) system. We need to point out that the GGA-PBE function usually overestimates the charge-transfer effects between interfaces and underestimates the band gaps for borophene and related 2D semiconductor materials, due to the well-known shortcoming of its self-interaction. This can be improved by using the hybrid functional like HSE or the many-body GW quasi-particle techniques.<sup>[43,44]</sup> Although the charge-transfer effects appear to be somewhat overestimated, the direction of charge transfer and its order of magnitude should not be substantially affected. Hence, the GGA-PBE calculated charge transfer in our study could be adequate to describe the weak boron–metal interactions. To gain a deeper insight into the boron–metal interactions, we analyzed the charge redistribution at the interface. Figure 4 presents the cross-section of the induced charge density difference between the interface and its individual components. All of the phases show a weak rearrangement of the charge density in the contact region (with an isovalue of only  $\approx 0.0025 \text{ e} \text{ \AA}^{-3}$ ), suggesting weak boron–silver binding. According to the relaxed geometries, the averaged distances between boron atoms and Ag substrate are all about 2.40 Å for three borophene phases, which is a typical distance for weak interaction between the boron sheets and Ag surface.<sup>[22]</sup> Additionally, the weak interface interaction is also reflected by the rather flat lattices of the three phases (see Figure 4) due to the absence of the interaction-induced out-of-plane buckling.

The perfect match between the period along the both types of chains (2.90 Å) and the lattice constant along the [110] direction of the Ag crystal (2.89 Å) is an important driving force for the formation of the (2,3) chains in the pure  $\beta_{12}$  phase and of the (2,2) chain in the  $\chi_3$  phase on the Ag surface.<sup>[22,23]</sup> However, as the (2,3) chains propagate along the  $[\bar{1}\bar{1}0]$  direction of Ag(100), the distance between the neighboring (2,3) chains in the pure  $\beta_{12}$  phases (5.0 Å) will have a large mismatch with the lattice constant of the Ag substrate (2.89 Å). To reduce the interface strain, the (2,2) chains with smaller lateral distance (4.3 Å) can be intercalated. In fact, with the intercalation of a single (2,2) chain between two (2,3) chains ((2,3):(2,2) = 2:1, i.e., phase A), the lattice periodicity of three chains shows a perfect match with five times the lattice constant of the  $[\bar{1}\bar{1}0]$  direction of Ag(100). Alternatively, four (2,3) chains are required to obtain the lattice spacing that matches five times the lattice constant of the  $[\bar{1}\bar{1}0]$  direction of Ag(100) (pure phase B). We calculated the average boron–boron bond lengths in the observed three phases, with the results shown in Table 1. The average bond

**Table 1.** Summary of the formation energy ( $E_f$ ), average charge per boron atom ( $Q_e$ ), and average bond lengths ( $\bar{L}$ ) of the experimentally synthesized borophene phases on Ag(100) surface and borophene phases on Ag(111) and freestanding borophene for comparison. Units of all parameters are given in the corresponding parentheses.

	Borophene on Ag(100)			Borophene on Ag(111)	Free-standing
	Type I – phase A (2,3):(2,2) = 2:1	Type I – phase B Pure $\beta_{12}$	Type II – phase C (2,3):(2,2) = 1:2	Pure $\beta_{12}$	Pure $\beta_{12}$
$E_f$ [eV/atom]	0.262	0.271	0.266	0.350	–
$Q_e$ [e/atom]	–0.019	–0.019	–0.022	–0.030	–
$\bar{L}$ [Å]	1.694	1.688	1.699	1.727	1.692

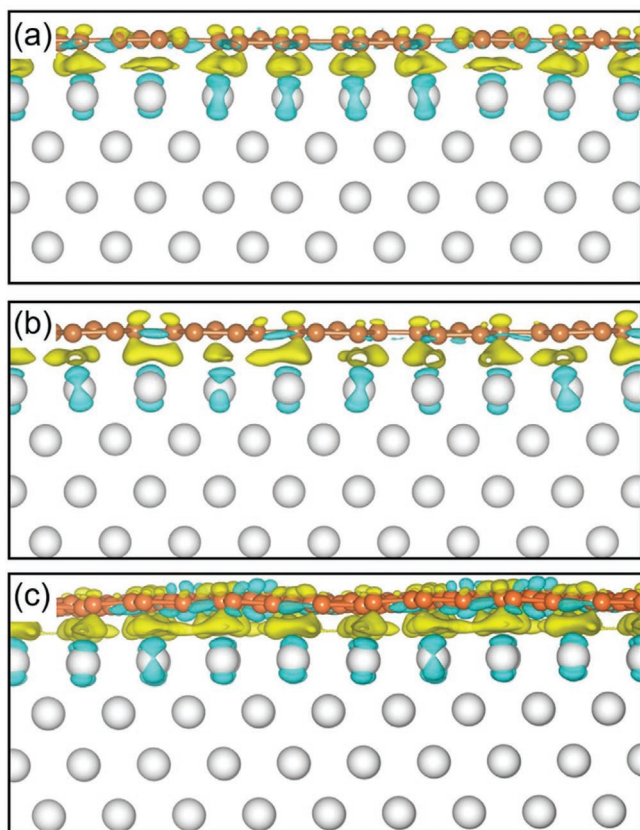


**Figure 4.** a–c) Isosurface of the differential charge density, defined as the difference between the total charge density of the borophene/substrate system and the sum of the total charge densities of the freestanding borophene sheet and the Ag(100) substrate at their original positions in the respective borophene/Ag(100) systems for phases A (a), phases B (b), and phase C (c). The yellow and cyan colors indicate electron accumulation and depletion, respectively. The red spheres and lines represent borophene, and the gray spheres show the Ag(100) substrate. The charge redistribution is visualized with an isovalue of  $0.0025 \text{ e } \text{Å}^{-3}$ .

lengths of the mixed phase A and pure phase B are 1.694 and 1.688 Å, respectively. It is clear that the former is closer to the calculated bond length (1.692 Å) for the freestanding  $\beta_{12}$  phase, suggesting that the mixed-chain phase suffers less strain accumulation and is more stable. Interestingly, the bond lengths in both A and B phases on Ag(100) are also closer to that of a freestanding  $\beta_{12}$  phase compared to the pure  $\beta_{12}$  phases on Ag(111) (Table 1), indicating that the mixed-chain phases on Ag(100) are much closer to the freestanding borophene forms. Together with the observed weaker charge transfer from the substrate to the phases on Ag(100), these results indicate that the mixed-chain phase is likely to be largely unaffected by the substrate and therefore will display the intrinsic physical properties of the borophene chains.

Furthermore, if additional (2,2) chains are intercalated between the (2,3) chains (i.e., phase C with the (2,3):(2,2) ratio of 1:2, the smaller lateral distance between the neighbor chains cannot match the lattice along the  $[1\bar{1}0]$  direction of Ag(100). Therefore, the mixed-chains must be rotated with respect to the substrate to obtain the optimal orientation for lattice matching.

That is to say, the borophene phases on Ag(100) with different proportions of the different chains can be well-separated based on the crystal direction of the substrate. However, the bond length of boron in phase C is larger than that of phase A, indicating that it is not as stable as phase A, and also explaining why only a small fraction of the surface is covered by the mixed-chain phase with the (2,3):(2,2) ratio of 1:2.

In summary, we have realized three types of long-range ordered phases of borophene on the Ag(100) surface. The STM measurements and DFT calculations reveal that two of these phases consist of the regular mixed arrangements of the (2,3) and (2,2) chains with ratios of 2:1 and 1:2, respectively. Theoretical calculations for the charge transfer and formation energy indicate that all borophene monolayers are planar and are weakly bound to the Ag(100) surfaces. Detailed structural analysis indicates that the matching of lattice parameters and orientation between the mixed boron chains and the Ag(100) surface play a crucial role in the formation of the mixed-chain phases. As a result, the mixed-chain phase with different chain ratios can be well separated based on the crystal directions of the substrate. It is important to note that the mixed-chain phases with long-range order suffer less strain than the pure phase borophene, suggesting that they may display the intrinsic physical properties theoretically predicted for the freestanding borophene form.

## Experimental Section

The experiments were performed in a homebuilt low-temperature STM with an MBE system (base pressure of  $\approx 10^{-10}$  Torr). Prior to boron growth, the single crystal Ag(100) substrate was cleaned by repeated cycles of  $\text{Ar}^+$  ion sputtering and annealing. Pure boron (powder, crystal, 99.999%) was evaporated from an e-beam evaporator onto the clean Ag(100) substrate maintained at  $\approx 550$  K. After growth, the sample was transferred to an STM chamber without breaking the vacuum. All of the STM images were taken at 5 K using a chemical etched W tip, and the bias voltages were defined as the tip bias with respect to the sample. The STM data were processed using the free WSxM software.<sup>[45]</sup>

**Computation:** All calculations based on DFT were carried out using the Vienna Ab initio Simulation Package (VASP).<sup>[46,47]</sup> The electron-ion interactions were described by the projector-augmented wave (PAW) method.<sup>[48]</sup> The generalized gradient approximation was chosen as implemented in the Perdew–Burke–Ernzerhof functional (GGA–PBE) to treat the exchange–correlation interactions of the electrons.<sup>[49]</sup> The plane-wave cutoff energy was set to 400 eV. The calculated models contain a boron monolayer on a four-layer Ag (100) surface with 12 Å of vacuum in the direction normal to the surface in order to eliminate the spurious interactions between the adjacent periodic images. The position of boron atoms and the Ag atoms of the top two layers were relaxed using the conjugate-gradient method until the force on each atom was less than  $0.01 \text{ eV } \text{Å}^{-1}$ . The Brillouin zone was sampled using a  $3 \times 15 \times 1$  k-point grid for the A and B borophene phases, and a  $3 \times 3 \times 1$  k-point grid for phase C borophene. The reason why different sampling was used for the calculations of borophenes' Brillouin zone is ensuring approximately the same k-point density among different-sized supercells for three types of borophene. The simulated STM images of these three types of borophene with different supercells were also performed using the VASP package within the Tersoff–Hamann approximation.<sup>[50]</sup> This code with the function of calculating the partial charge density, can be used to obtain the local density of states (LDOS) by the wavefunctions in the energy windows  $[E_{\text{Fermi}} - eV_{\text{bias}}, E_{\text{Fermi}}]$ . The energy ranges of DFT-simulated constant current mode STM are 0–1.6 eV for A and B borophene phases, 0–0.5 eV for C borophene phase, respectively.

## Acknowledgements

Y.W. and L.K. contributed equally to this work. This work was financially supported by Ministry of Science and Technology of China (2018YFE0202700, 2016YFA0300904, 2016YFA0202301), National Natural Science Foundation of China (11674366, 11761141013, 11674368, 11825405), Beijing Municipal Natural Science Foundation (Z180007), and Chinese Academy of Sciences (XDB30000000).

## Conflict of Interest

The authors declare no conflict of interest.

## Keywords

borophene, long-range order, mixed phases, molecular beam epitaxy, phase separation, quasi-1D chains

Received: July 28, 2020

Revised: September 29, 2020

Published online:

- [1] P. Vogt, P. D. Padova, C. Quaresima, J. Avila, E. Frantzeskakis, M. C. Asensio, A. Resta, B. Ealet, G. L. Lay, *Phys. Rev. Lett.* **2012**, *108*, 155501.
- [2] B. J. Feng, Z. J. Ding, S. Meng, Y. G. Yao, X. Y. He, P. Cheng, L. Chen, K. H. Wu, *Nano Lett.* **2012**, *12*, 3507.
- [3] L. Chen, C. C. Liu, B. J. Feng, X. Y. He, P. Cheng, Z. J. Ding, S. Meng, Y. G. Yao, K. H. Wu, *Phys. Rev. Lett.* **2012**, *109*, 056804.
- [4] M. E. Dávila, L. Xian, S. Cahangirov, A. Rubio, G. L. Lay, *New J. Phys.* **2014**, *16*, 095002.
- [5] L. F. Li, S. Z. Lu, J. B. Pan, Z. H. Qin, Y.-Q. Wang, Y. L. Wang, G.-Y. Cao, S. X. Du, H.-J. Gao, *Adv. Mater.* **2014**, *26*, 4820.
- [6] L. K. Li, Y. J. Yu, G. J. Ye, Q. Q. Ge, X. D. Ou, H. Wu, D. L. Feng, X. H. Chen, Y. B. Zhang, *Nat. Nanotechnol.* **2014**, *9*, 372.
- [7] F.-F. Zhu, W.-J. Chen, Y. Xu, C.-L. Gao, D.-D. Guan, C.-H. Liu, D. Qian, S.-C. Zhang, J.-F. Jia, *Nat. Mater.* **2015**, *14*, 1020.
- [8] J. Gou, L. J. Kong, H. Li, Q. Zhong, W. B. Li, P. Cheng, L. Chen, K. H. Wu, *Phys. Rev. Mater.* **2017**, *1*, 054004.
- [9] X. C. Huang, J. Q. Guan, Z. J. Lin, B. Liu, S. Y. Xing, W. H. Wang, J. D. Guo, *Nano Lett.* **2017**, *17*, 4619.
- [10] L. J. Kong, K. H. Wu, L. Chen, *Front. Phys.* **2018**, *13*, 138105.
- [11] D. F. Li, J. F. Gao, P. Cheng, J. He, Y. Yin, Y. X. Hu, L. Chen, Y. Cheng, J. J. Zhao, *Adv. Funct. Mater.* **2020**, *30*, 1904349.
- [12] T. R. Galeev, Q. Chen, J.-C. Guo, H. Bai, C.-Q. Miao, H.-G. Lu, A. P. Sergeeva, S.-D. Li, A. I. Boldyrev, *Phys. Chem. Chem. Phys.* **2011**, *13*, 11575.
- [13] H. Tang, S. Ismail-Beigi, *Phys. Rev. Lett.* **2007**, *99*, 115501.
- [14] H. Tang, S. Ismail-Beigi, *Phys. Rev. B* **2010**, *82*, 115412.
- [15] E. S. Penev, S. Bhowmick, A. Sadrzadeh, B. I. Yakobson, *Nano Lett.* **2012**, *12*, 2441.
- [16] X. J. Wu, J. Dai, Y. Zhao, Z. W. Zhuo, J. L. Yang, X. C. Zeng, *ACS Nano* **2012**, *6*, 7443.
- [17] H. S. Liu, J. F. Gao, J. J. Zhao, *Sci. Rep.* **2013**, *3*, 3238.
- [18] X. B. Yang, Y. Ding, J. Ni, *Phys. Rev. B* **2008**, *77*, 041402(R).
- [19] Y. Y. Liu, E. S. Penev, B. I. Yakobson, *Angew. Chem., Int. Ed.* **2013**, *52*, 3156.
- [20] Z. H. Zhang, Y. Yang, G. Y. Gao, B. I. Yakobson, *Angew. Chem., Int. Ed.* **2015**, *54*, 13022.
- [21] A. J. Mannix, X.-F. Zhou, B. Kiraly, J. D. Wood, D. Alducin, B. D. Myers, X. L. Liu, B. L. Fisher, U. Santiago, J. R. Guest, M. J. Yacaman, A. Ponce, A. R. Oganov, M. C. Hersam, N. P. Guisinger, *Science* **2015**, *350*, 1513.
- [22] B. J. Feng, J. Zhang, Q. Zhong, W. B. Li, S. Li, H. Li, P. Cheng, S. Meng, L. Chen, K. H. Wu, *Nat. Chem.* **2016**, *8*, 563.
- [23] Q. Zhong, J. Zhang, P. Cheng, B. J. Feng, W. B. Li, S. X. Sheng, H. Li, S. Meng, L. Chen, K. H. Wu, *J. Phys. Condens. Matter* **2017**, *29*, 095002.
- [24] Q. Zhong, L. J. Kong, J. Gou, W. B. Li, S. X. Sheng, S. Yang, P. Cheng, H. Li, K. H. Wu, L. Chen, *Phys. Rev. Mater.* **2017**, *1*, 021001(R).
- [25] W. B. Li, L. J. Kong, C. Y. Chen, J. Gou, S. X. Sheng, W. F. Zhang, H. Li, L. Chen, P. Cheng, K. H. Wu, *Sci. Bull.* **2018**, *63*, 282.
- [26] B. Kiraly, X. L. Liu, L. Q. Wang, Z. H. Zhang, A. J. Mannix, B. L. Fisher, B. I. Yakobson, M. C. Hersam, N. P. Guisinger, *ACS Nano* **2019**, *13*, 3816.
- [27] R. T. Wu, I. K. Drozdov, S. Eltinge, P. Zahl, S. Ismail-Beigi, I. Božović, A. Gozar, *Nat. Nanotechnol.* **2019**, *14*, 44.
- [28] N. A. Vinogradov, A. Lyalin, T. Taketsugu, A. S. Vinogradov, A. Preobrajenski, *ACS Nano* **2019**, *13*, 14511.
- [29] L. J. Kong, L. R. Liu, L. Chen, Q. Zhong, P. Cheng, H. Li, Z. H. Zhang, K. H. Wu, *Nanoscale* **2019**, *11*, 15605.
- [30] B. J. Feng, J. Zhang, R.-Y. Liu, T. Iimori, C. Lian, H. Li, L. Chen, K. H. Wu, S. Meng, F. Komori, I. Matsuda, *Phys. Rev. B* **2016**, *94*, 041408(R).
- [31] X.-F. Zhou, X. Dong, A. R. Oganov, Q. Zhu, Y. J. Tian, H.-T. Wang, *Phys. Rev. Lett.* **2014**, *112*, 085502.
- [32] B. J. Feng, O. Sugino, R.-Y. Liu, J. Zhang, R. Yukawa, M. Kawamura, T. Iimori, H. Kim, Y. Hasegawa, H. Li, L. Chen, K. H. Wu, H. Kumigashira, F. Komori, T.-C. Chiang, S. Meng, I. Matsuda, *Phys. Rev. Lett.* **2017**, *118*, 096401.
- [33] Y. C. Zhao, S. Zeng, J. Ni, *Phys. Rev. B* **2016**, *93*, 0145021.
- [34] Z. H. Zhang, Y. Yang, E. S. Penev, B. I. Yakobson, *Adv. Funct. Mater.* **2017**, *27*, 1605059.
- [35] H. B. Zhou, Y. Q. Cai, G. Zhang, Y.-W. Zhang, *npj 2D Mater. Appl.* **2017**, *1*, 14.
- [36] Z. H. Zhang, E. S. Penev, B. I. Yakobson, *Chem. Soc. Rev.* **2017**, *46*, 6746.
- [37] N. G. Szwacki, A. Sadrzadeh, B. I. Yakobson, *Phys. Rev. Lett.* **2007**, *98*, 166804.
- [38] X. L. Liu, Z. H. Zhang, L. Q. Wang, B. I. Yakobson, M. C. Hersam, *Nat. Mater.* **2018**, *17*, 783.
- [39] X. L. Liu, L. Q. Wang, S. W. Li, M. S. Rahna, B. I. Yakobson, M. C. Hersam, *Nat. Commun.* **2019**, *10*, 1642.
- [40] D. Y. Geng, K. J. Yu, S. S. Yue, J. Cao, W. B. Li, D. S. Ma, C. X. Cui, M. Arita, S. Kumar, E. F. Schwier, K. Shimada, P. Cheng, L. Chen, K. H. Wu, Y. G. Yao, B. J. Feng, *Phys. Rev. B* **2020**, *101*, 161407(R).
- [41] Z. H. Zhang, E. S. Penev, B. I. Yakobson, *Nat. Chem.* **2016**, *8*, 525.
- [42] Z. H. Zhang, S. N. Shirodkar, Y. Yang, B. I. Yakobson, *Angew. Chem., Int. Ed.* **2017**, *129*, 15623.
- [43] L. Adamska, S. Sadasivam, J. J. Foley IV, P. Darancet, S. Sharifzadeh, *J. Phys. Chem. C* **2018**, *122*, 4037.
- [44] S. Pari, A. Cuellar, B. M. Wong, *J. Phys. Chem. C* **2016**, *120*, 18871.
- [45] I. Horcas, R. Fernández, J. M. Gómez-Rodríguez, J. Colchero, J. Gómez-Herrero, A. M. Baro, *Rev. Sci. Instrum.* **2007**, *78*, 013705.
- [46] G. Kresse, J. Furthmüller, *Phys. Rev. B* **1996**, *54*, 11169.
- [47] G. Kresse, J. Furthmüller, *Comput. Mater. Sci.* **1996**, *6*, 15.
- [48] G. Kresse, D. Joubert, *Phys. Rev. B* **1999**, *59*, 1758.
- [49] J. P. Perdew, K. Burke, M. Ernzerhof, *Phys. Rev. Lett.* **1996**, *77*, 3865.
- [50] J. Tersoff, D. R. Hamann, *Rhys. Rev. Lett.* **1983**, *50*, 1988.